Low to very high temperature thermal energy recycling – 3 case studies

Arne Høeg[1,*], *Tor-Martin* Tveit[2]

[1]Enerin AS, Evja Vest, NO-6900 Florø, Norway
[2]Åbo Akademi University, Biskopsgatan 8, FI-20500 Åbo, Finland

Abstract. In this paper we present three case studies of the installation of a stirling-cycle high temperature heat pump applied to recycling thermal energy including steam generation.

Many industries have heat demand at temperatures above 100°C and often the preferred energy carrier is steam. The optimal integration of a heat pump can be determined by investigating the thermal need of the process with pinch technology. For many industries, the pinch temperature is too high for conventional heat pumps. We present a heat pump solution that can recycle thermal energy and deliver this to a heat source up to 200°C, as hot water or steam. The heat pump can be integrated in a thermodynamic efficient way placing the sink and source in-between the pinch temperature. The working medium is a gas throughout the process cycle, with no evaporation or condensation. Thus, the process can auto-adjust to temperature variations and achieve very high efficiencies compared to the Carnot heat pump cycle. The coefficient of performance (COP) of the heat pump vary with the sink/source temperatures as the temperature fraction varies. Another important feature is that the medium has both a global warming potential (GWP) and ozone depletion potential (ODP) of zero. The thermodynamics of the heat pump is explained in more detail in the introduction section.

The first installation is at a dairy plant on the west coast of Norway. In this installation, the heat pump provides cooling at 0-5°C and converts this heat into hot water at 120°C. The second installation is also at a dairy in Norway. Here the heat pump cools the ammonia from the cooling compressors at about 25-30°C and converts the heat to hot water at 110C°. The third installation is at a beverage plant on the west coast of Norway. Here the heat pump is providing cooling to compressors and other equipment. The final temperature of the heat source varies from 20-70°C. The heat is converted into steam at 168°C. In the case study sections, the installations are discussed in more details, together with the performance and a discussion of the experiences with the technology.

* Corresponding author: arne@hoeg.no

1 Introduction

The ability to lift heat at high temperatures and at high temperature lifts, gives the heat pump more options for industrial use. I many industries, the main heat demand is above 100°C and being able to deliver heat in this temperature range increases the potential use of heat pumps.

The next sections will describe the theory behind the heat pump process and how the heat pump performance is estimated. The last sections will give an overview of the cases and a detailed description of the performance of the heat pumps based on onsite measurements.

1.1 Heat pump process description

The most common heat pump technologies today are not designed for high temperatures or high temperature lifts. The heat pump process presented in this paper is based on the Stirling cycle. The modern Stirling engine starts with the work done by Philips Electronics BV in the Netherlands in the 1940ies. See for instance the book by (Finkelstein and Organ, 2001) for a historical review of the modern Stirling engine. The ideal Stirling cycle is a thermodynamic process that consists of four reversible process in series. A description of the ideal Stirling cycle is available in most introductions to technical thermodynamics, for instance in the book by (Moran and Shapiro, 1993).

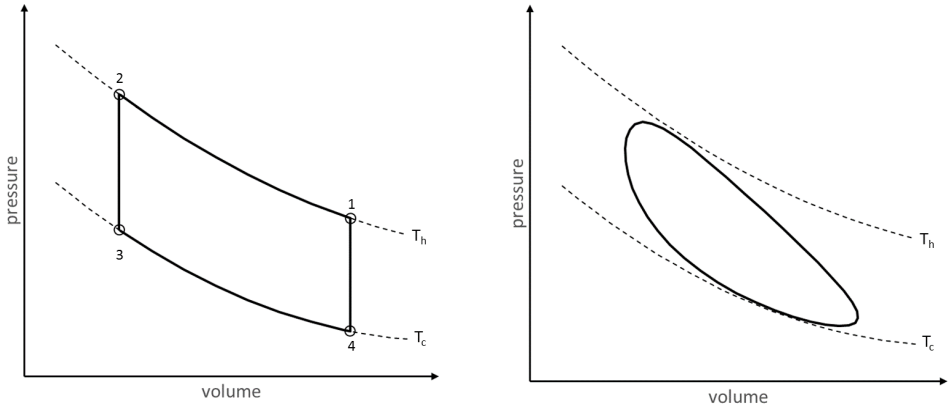

(a) Ideal Stirling cycle in a p-v diagram. State 1→2 isothermal compression, state 2→3 constant volume cooling, state 3→4 isothermal expansion and 4→2 constant volume heating.

(b) Real Stirling cycle based heat pump cycle in a p-v diagram. The motion of the reciprocating pistons approximates the ideal state changes of the working medium.

Fig.1. The ideal Stirling cycle (a) compared to the real heat pump cycle (b) in p-v diagrams. The real cycle is based on a simulation model of the heat pump with parameters matching the actual parameters of one of the installed heat pumps

In fig.1. an ideal and a real Stirling process are shown in p-v diagrams. Compared to compression and absorption heat pumps, the working medium in a Stirling process is a gas throughout the process. This means that the process is independent of the evaporation and condensation temperatures of the working medium. A common question from persons not familiar with the Stirling process is related to the choice of working medium. Even though, the full story is more complicated, the efficiency of the choice of working medium can easily be seen from the equation below. Equation 1 shows an expression for the work of an ideal Stirling cycle by an ideal gas.

$$w = -mR\ln\left(\frac{V_1}{V_2}\right)(T_h - T_c) \quad (1)$$

where m is the mass of the working medium, R is the specific gas constant of the working medium, V is the volume, and T is the temperature. The subscripts "1" and "2" refere to the states in fig.1. a. As can be seen from the equation, the higher the value of the specific gas constant, the higher the work output from the cycle. Noting that the specific gas constant for hydrogen, helium and air are approximately 4000, 2100 and 300 J/kgK respectively, it is easily understood why hydrogen and helium are prefered working media to air or nitrogen. The same argument is also valid for the reverse (heat pump) Stirling cycle.

1.2 Working Principle of the Heat Pump

The configuration of the heat pump is a double-acting alpha Stirling engine of the "Franchot" type. The "double-acting" means that the working medium is acting on both sides of the pistons. The figure below shows the principle behind the configuration.

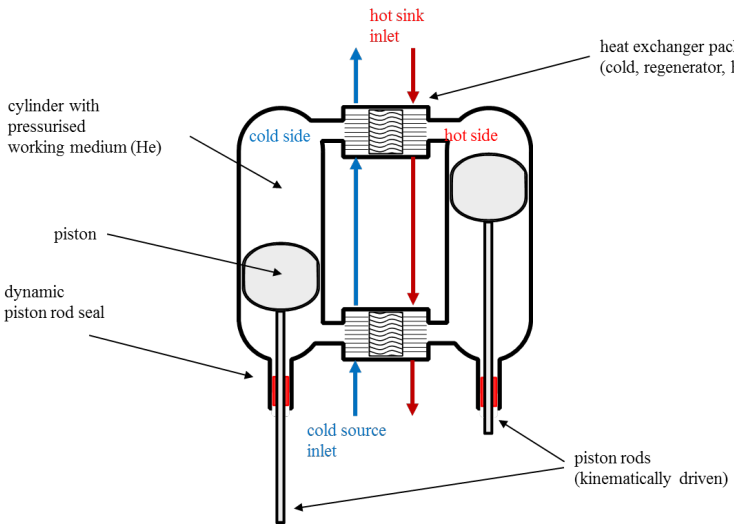

Fig.2. Schematic overview of the heat pump configuration. Two pistons move phase shifted to each other (with respect to the crank angle). The two pistons work together to move the gas from one side of the heat pump to the other, and to compress and expand the gas. When most of the gas is in the hot side of the heat pump the pistons compress the gas and when most of the gas is in the cold side, the pistons expand the gas

The Franchot type means in contrast to a "Rinia" or "Siemens" type configuration, one of the cylinders is always containing cold gas and one of the cylinders is always containing hot gas.

2 Heat pump performance estimation

The Stirling cycle is an inherit dynamic process that can be described as cyclic steady state. Many simplified models of estimating the performance of Stirling engines have been developed. A description of earlier developments of Stirling cycle models can be found in the book by (Martini, 1983/2004). However, for more accuracy the resulting model will

consist of a stiff set of differential equations, which in many cases are very difficult to solve. The approach used by the author is to build a finite volume model of the Stirling process in Sage by (Gedeon, 2009). The model takes into account many thermodynamic and fluid mechanical losses. Additional mechanical and thermal losses are superimposed on the results of the model to better match the real behavior of the heat pump. More details regarding the process design of the heat pump can be found in the previous work by the authors (Høeg and Tveit, 2018).

In order to get a map of the performance of the heat pump, the simulation model of the heat pump has been solved for various combinations of the sink and source temperatures. For heat engines the main dimensionless parameter is the cold temperature divided by the hot temperature in Kelvin, Tc/Th. Plotting the share of the calculated Coefficient of Performance (COP) of the theoretical optimal COP, the Carnot COP, as a function of the temperature fraction gives a two-dimensional performance map. The advantage of using these parameters is that it is possible to plot a large number of different combinations of conditions in one graph. The performance map for the SPP 4 106 series is shown in the figure below.

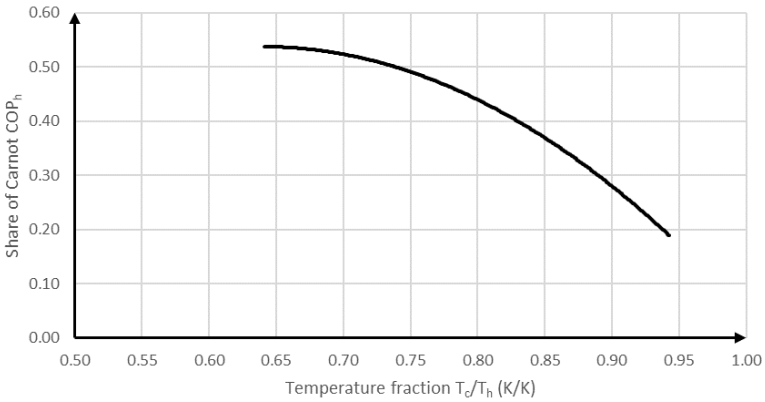

Fig.3. Performance map of the SPP 4 106-series. The temperature fraction is the cold source temperature, Tc, divided by the hot sink temperature, Th, in degrees Kelvin. The performance map is generated from simulations of the process.

As can be seen from the performance map, the "sweet spot" for the SPP 4 106 series is for temperature fractions between 0.65 and 0.75. A temperature fraction of 0.65 could for instance correspond to a cold source temperature of 0°C and a hot sink of 150°C, while a temperature fraction of 0.75 could be correspond to cold and hot temperatures of 50°C and 155°C respectively. The Beale-numbers for typical operation points for the three heat pumps are shown in the table below:

Table 1. Beale numbers for three operationg points

		TINE Byrkjelo	TINE Frya	Lerum
Beale number	$N_B = W/(p_{ref} V_{sw})$	5.5	7.4	5.6

The differences in the Beale-numbers are mainly due to the various shaft speeds, 400-650 r/min, but the operating hot and cold temperatures also affect the power from the main motor. In addition, there are differences in the swept volume of the heat pumps. This is explained further in the previous work by the authors (Høeg and Tveit, 2018).

3 Cases

The heat pump has been installed at three different sites with different heating and cooling demands. The cases are as follows:

- TINE Meieriet Byrkjelo: A dairy plant in Norway that produces cheese and milk. Processes about 130 million litres of raw milk every year.
- TINE Meieriet Frya: A dairy plant in Norway that produces yogurt and cottage cheese. The annual production is about 50 million litres.
- Lerum Fabrikker: Juice, beverages and jam factory in Norway. The factory is family owned since 1907.

The figure below shows the sink/source temperatures for the three installations.

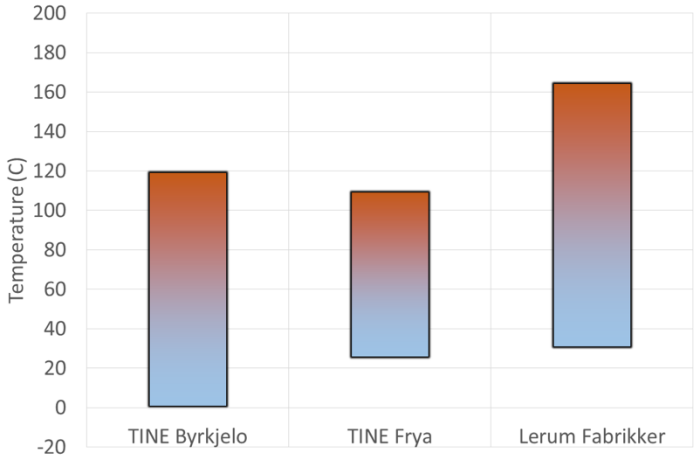

Fig.4. Overview of the temperature lift (difference between the sink and source temperatures) at the different cases. These are the design temperatures, the actual temperatures shows various degrees of fluctuation.

The following sections give an overview of the different installations and the performance of the heat pumps.

3.1 Case 1. Dairy Plant TINE Meieriet Byrkjelo

The heat pump at TINE Meieriet Byrkjelo is the first commercial installation of SPP HighLift heat pumps. The heat pump is simultaneously generating hot water at 120°C and cooling at 0°C at the design point. The figure below shows the simplified P&ID of the installation.

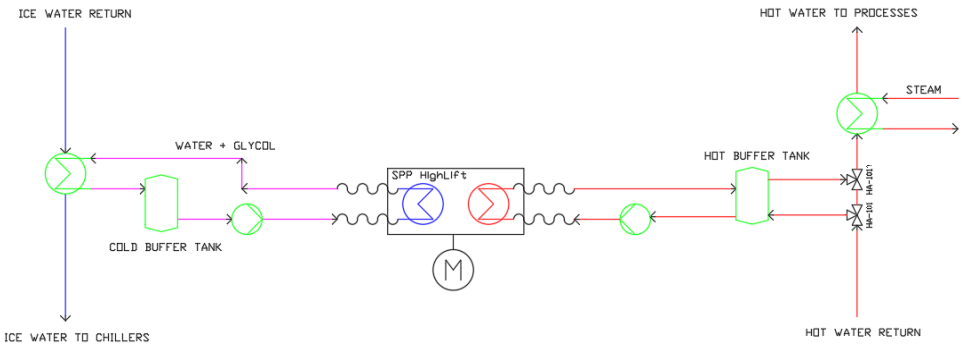

Fig.5. Simplified P&ID of the heat pump installation at TINE Byrkjelo. The hot water return temperature can fluctuate from 80° to 120°C during a day. The ice water return temperatures are stable at around 3-4° C within a few degrees during a day, but show more seasonal variation.

Since the temperature of the water used for cooling, ice water, is close to the freezing point, a closed intermediate circuit of water and glycol is used to reduce the risk of freezing in the internal heat exchangers of the heat pump. In the cases where the heat pump is unable to heat the water to the required temperature, there is an additional steam heat exchanger in series with the heat pump. The figure below shows a photo of the installation.

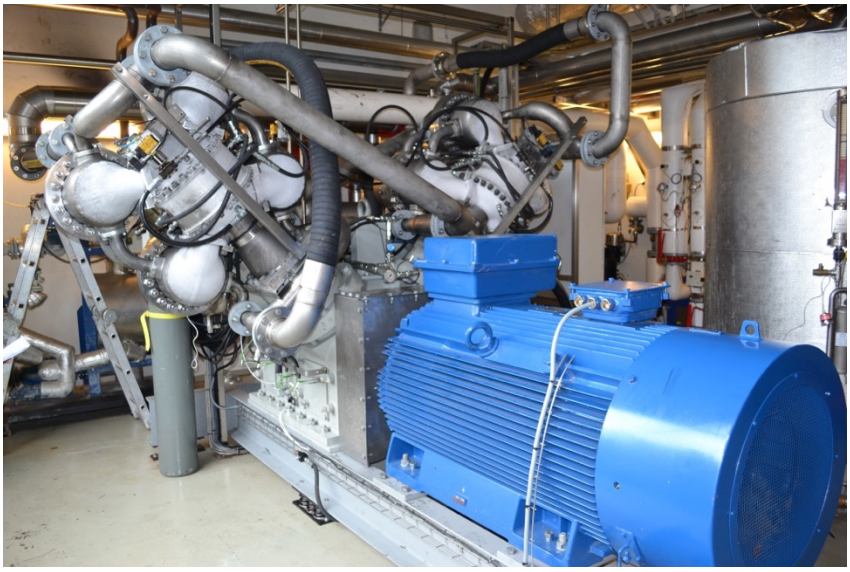

Fig.6. HighLift heat pump model SPP 4 106A at TINE Meieriet Byrkjelo, Norway. The icy, cold cylinders are facing the camera, while the hot cylinders (120°C) are facing the wall.

One interesting feature of the HighLift heat pump is that it will automatically adapt to even rapid changes in the temperatures of the sink and source. This can be seen at the installation in TINE Meieriet Byrkjelo, where the return temperature of the hot water from the processes varies between 80° to 120°C during a day. The changes can also be very rapid. The figure below shows a time series of the return temperature of the hot water during a week.

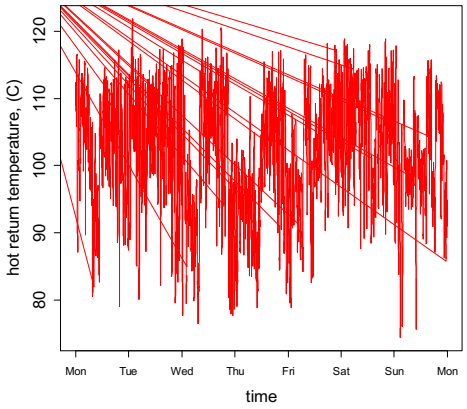

(a) Time series of the return temperature of the hot water from the processes. The changes are caused by the starting and ending of batch processes and equipment cleaning.

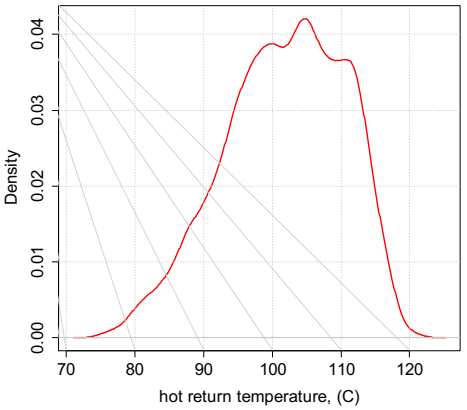

(b) Distribution of the return temperature for the time series shown in (a).

Fig.7. The return water from the processes shows large temperature variations during the days. The variations are typical for the installation and are caused by the production scheduling. There are very little seasonal variations in the temperature.

For a heat pump that is sensitive to the conditions, a degradation in the heat duty or and non-linear increase in the power consumption. The figure below shows the main motor power consumption and heat duty as a function of the return temperature of the hot water. The mass flow used to estimate the heat flow has been calculated according to the specification of the circulation pump.

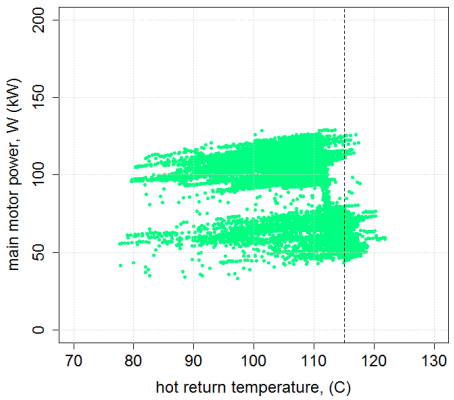

(a) Main motor power as a function of the inlet temperature of the hot water to the heat pump (return water).

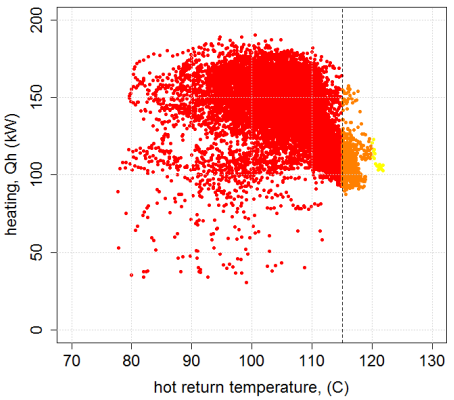

(b) Heat delivered to the hot water as a function of the inlet temperature of the hot water to the heat pump (return water).

Fig.8. Motor power and heating as a function of the inlet temperature of the hot water for the periods when the heat pump was running during the week (103 hours). The heat pump is set to reduce the power when the temperature is closing 115°C.

The division into two clusters that can be seen in the figures is due to the automatic load control of the heat pump. The reduction in power is either caused by lower heat demand or lower cooling demand. If either demand goes below the range of the heat pump, the heat pump shuts down automatically and starts when the heat demand again is above the threshold. The figure below shows the Coefficient of Performance for the period.

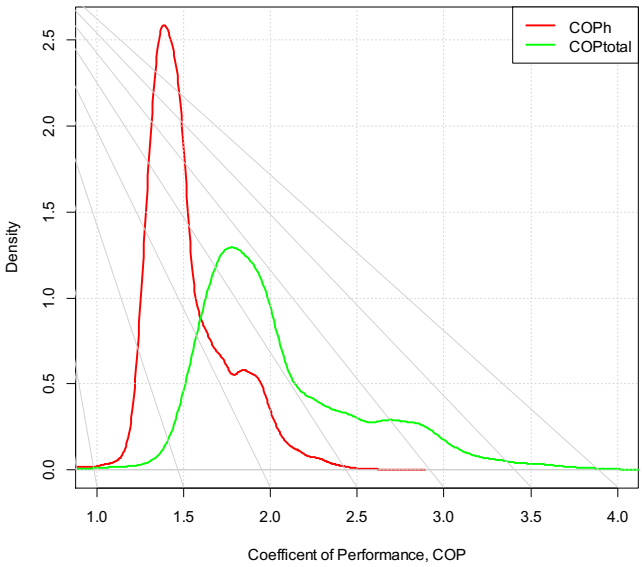

Fig.9. Distribution of the heating Coefficient of Performance, COP_h, and the total Coefficient of Performance, COP_{total}, for a typical week. The mean COP_h is 1.53 and the mean COP_{total} is 2.06.

A comparison between the performance shown and the ideal Carnot heat pump is given in the figure below.

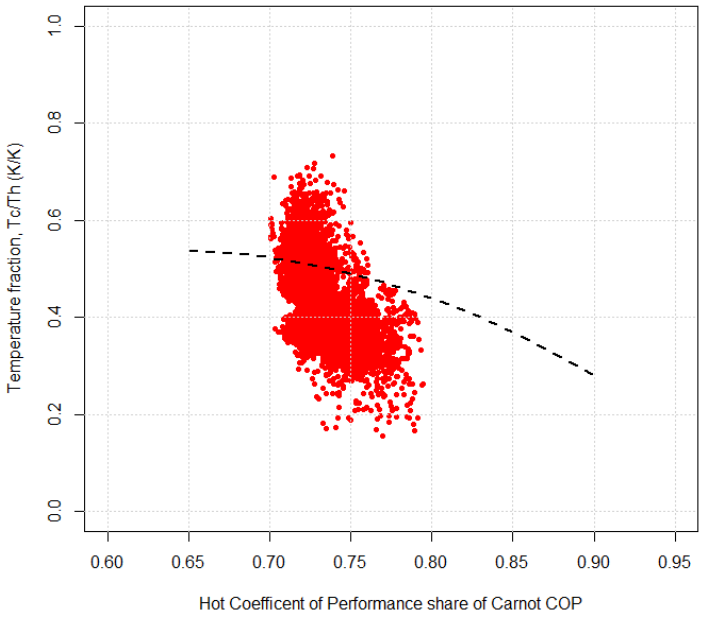

Fig.10. Comparison of the real and ideal performance of the heat pump. The simulation based estimation of the performance is shown in the dotted line. The large variation in the COP_h is caused by thermal intertia

As can be seen from the figure, the simulation based estimation is a good approximation. However, there is a large spread of the performance. This spread can be explained by thermal inertia. If the temperature of the hot water is decreasing and increase in the heat flow will be caused by the cooling of the heat pump and not by the heat pump process. In this case the COP will be higher than would be expected by the process. Similarly, if the temperature is increasing, heat from the heat pump process is used to heat the heat pump and subsequently less heat is transferred to the hot water.

3.2 Case 2. Dairy Plant TINE Meieriet Frya

The heat pump at TINE Meieriet Frya pre-cools the ammonia from the chillers and lifts the heat to 110°C. The hot side of the heat pump is in series with the electric boiler. In order to have a sufficient heat transfer, the ammonia is cooled in a heat exchanger that is connected to a closed water circuit that circulate water over the heat pump. The figure below shows a simplified P&ID of the installation.

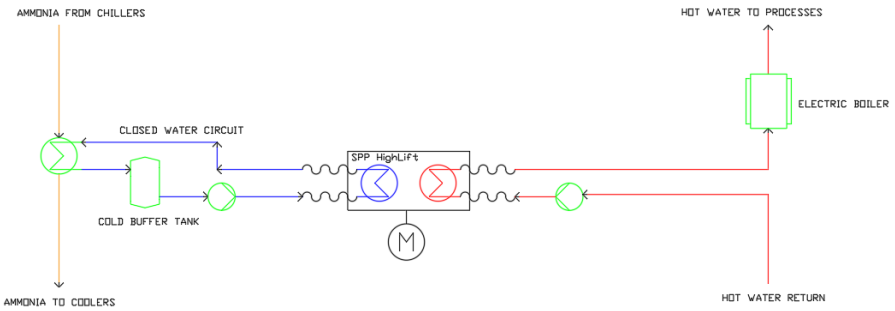

Fig.11. Simplified P&ID of the heat pump installation at TINE Meieriet Frya. The heat source is ammonia from the chillers that is precooled in a heat exchanger connected to the heat pump. The hot sink is hot water that is preheated before an electric boiler.

The figure below shows a photo of the installation at TINE Meieriet Frya.

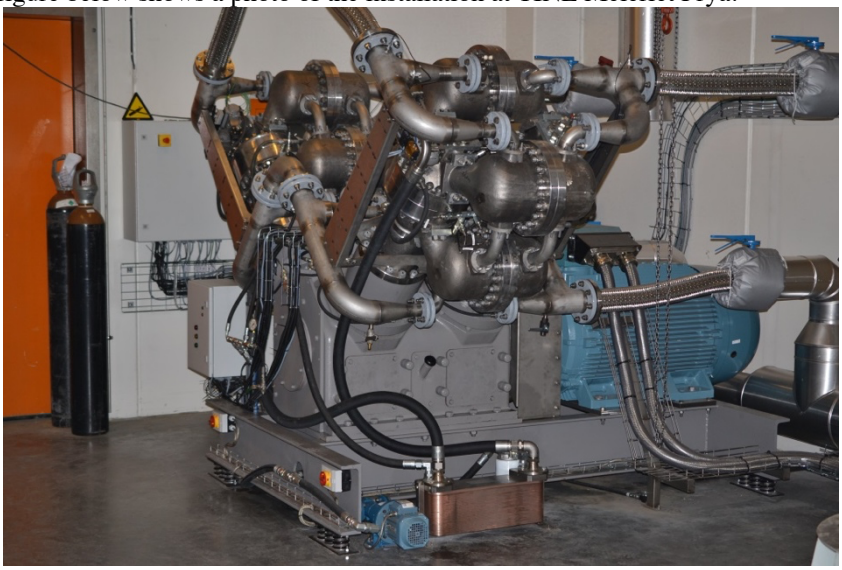

Fig.12. HighLift heat pump model SPP-4-106B at TINE Frya, Norway. The cold side is out towards the left, while the hot side is facing the wall on the right side of the photograph. Both the heat source and heat sink are connected to the heat pump using flexible hoses to isolate any vibrations.

The performance of the heat pump at TINE Meieriet Frya is documented in the previous work (Tveit and Høeg, 2014). The performance was documented for three different cases shown in the table below.

Table 2. Summary of performance measurements for three cases at TINE Meieriet Frya, where case 1-3 corresponds to loads of 54%, 84% and 100% respectively.

Parameter	Symbol and unit	Case #1	Case #2	Case #3
Average cold temperature	T_c (°C	27	26	27
Average hot temperature	T_{tank} (°C)	106	105	105
Coefficient of Performance	COP_h	2.00	2.20	2.00
Carnot COP	COP_{carnot}	4.80	4.78	4.85
Share of Carnot COP	COP_h/COP_{carnot}	42%	46%	41%
Overall COP	COP_{tot}	3.1	3.5	3.1

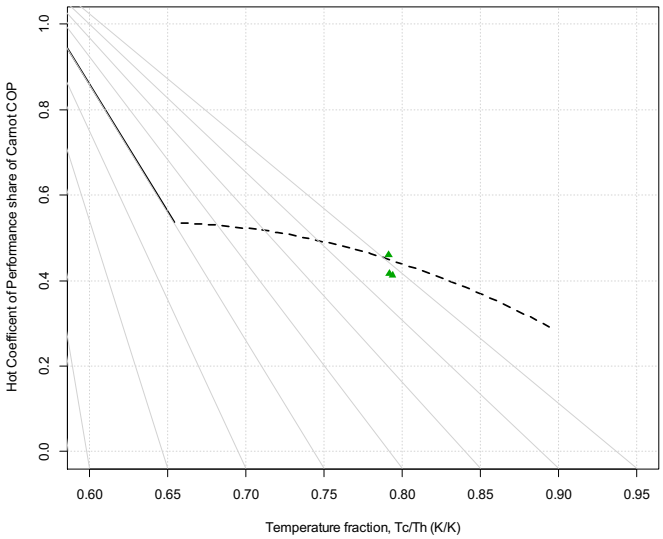

Fig.13. Performance of SPP-4-106 at TINE Meieriet Frya compared to the estimated heat pump performance as share of Carnot Coefficient of Performance.

3.3 Case 3. Juice and Beverage Plant Lerum Fabrikker

At the time of writing the heat pump at Lerum Fabrikker in Norway is generating steam at 0.65 MPa (gauge) using heat from the oil of cooling compressors as a heat source. A second heat pump is planned installed at the site when additional processes are added to the site. The figure below shows a simplified P&ID of the installation.

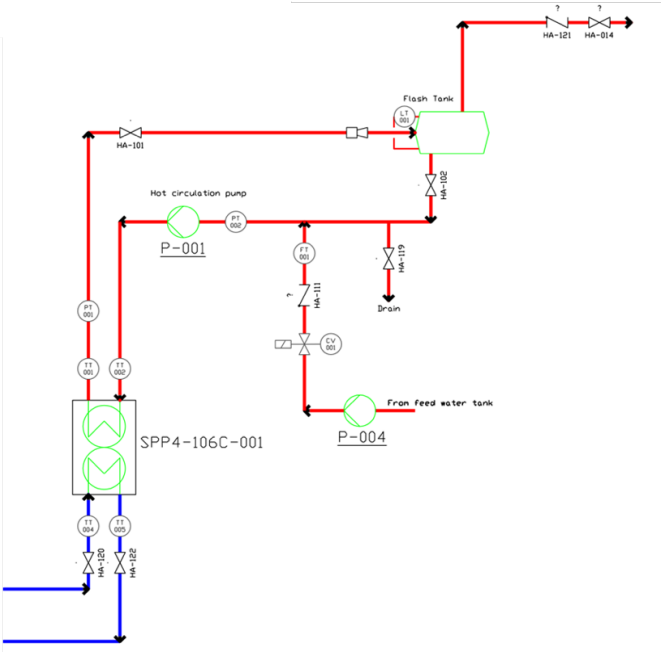

Fig.14. Simplified P&ID of the heat pump installation at Lerum Fabrikker. Feedwater enters the system in the lower right and steam exits the system at the upper right. Waste heat is entering and exiting in the lower left.

To avoid the risk of cavitation on internal heat exchanger of the heat pump, the pressure of the saturated water from the flash tank is increased with approximately 0.40 MPa. After the water is heated by the heat pump the pressure is reduced by a perforated plate at the inlet to the flash tank. There is a check valve between the flash tank and the steam system at the plant, which makes sure that the steam is only entering the system when it is at the correct pressure.

The picture below shows the installation in the engine room.

Fig.15. HighLift heat pump model SPP 4-106C at Lerum Fabrikker, Norway. The main drive and drives for auxiliary equipment are shown on the left, while the flash tank for steam generation can be seen in the upper right corner.

There is no continuous measurement of the flow of the feedwater, but a pulse meter that register every 10 litre of flow. During a time period, Δt, the heat flow can be estimated according to the following equation (thermal losses ignored):

$$Q_h \approx \frac{Q_{steam} + Q_{feed}}{\Delta t} = \frac{m \cdot (h_{fg} + c_p \cdot (T_{steam} - T_{feed}))}{\Delta t} \quad (2)$$

where Q_{steam} is the heat needed to evaporate the steam and Q_{feed} is the heat needed to heat the feedwater from the temperature in the feedwater tank to the saturation temperature. Furthermore, m is the total flow of feedwater in the period, h_{fg} is the specific heat of evaporation, T_{steam} is the saturation temperature and T_{feed} is the temperature of the feedwater. In order to measure the performance two periods where the operating conditions were stable for a long time was chosen. For Case #1 the conditions were stable for about 200 minutes and for Case #2 for about 100 minutes. This gives 3000 and 6000 operating points respectively. The table below shows a summary of the performance measurements and calculations.

Table 3. Summary of performance measurements and calculation for two different operating conditions for SPP 4 106C at Lerum Fabrikker. The main difference between Cases #1 and #2 is the temperature of the cold heat source.

Parameter	Symbol and unit	Case #1	Case #2
Average cold temperature	T_c (°C	23	33
Average tank pressure	p_{tank} (bar_g)	6.3	6.3
Average tank temperature	T_{tank} (°C)	167	167
Feed water temperature	T_{fw} (°C)	90	90
Energy for feed water heating	E_{fw} (kJ)	251 573	170 821
Energy for steam generation	E_{steam} (kJ)	1 611 241	1 094 052
Periode in minutes	t (min)	206	100
Total average heat power	Q_h (kW)	151	211
Average power consumption	W (kW)	106	140
Coefficient of Performance	COP_h	1.42	1.51
Carnot COP	COP_{carnot}	3.06	3.29
Share of Carnot COP	COP_h/COP_{carnot}	46%	46%
Estimated cooling	Q_c (kW)	65	91
Overall COP	COP_{tot}	2.0	2.2

The share of Carnot Cofficient of Performance for the two cases is lower than can be expected when looking at the performance chart in Figure 3. The performance chart includes various internal losses, but not heat loss from the piping and flash tank. An estimation of the heat loss from the piping not accounted for in the model, gives about 13 kW of additional heat. About 50% of the heat loss can be attributed to convection and 50% to radiation. The performance with and without the additional heat loss estimation is presented in the figure below.

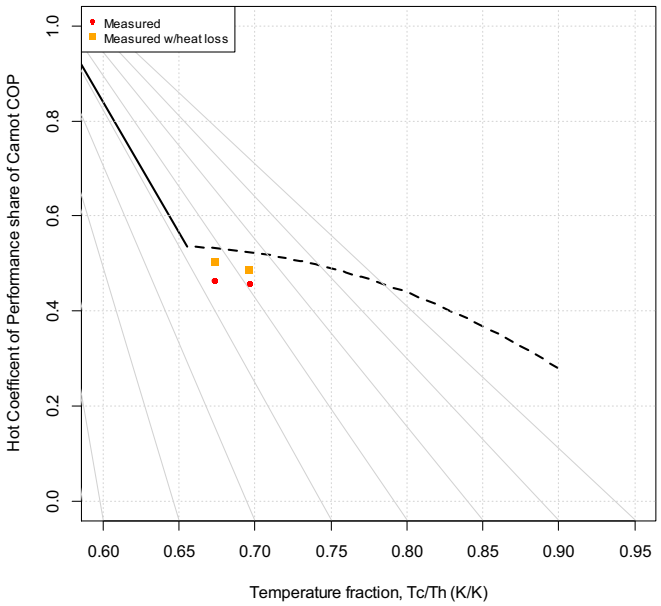

Fig.16. Performance of SPP 4-106C compared to the estimated heat pump performance as share of Carnot Coefficient of Performance.

Considering the probable accuracy of the loss estimation, the figure shows a good correspondence with the estimated performance.

4 Discussion and Conclusions

The results of the case study show that the estimated performance of the heat pump aligns well with the measurements of the performance of the installations. This is an important result, which will make it easier to calculate the feasibility of other applications of the heat pump. In addition, the results show that SPP 4-106 HighLift heat pump is a very versatile heat pump suited for combined heating and cooling as well as steam generation. The heat pump is well adapted to changing operating conditions.

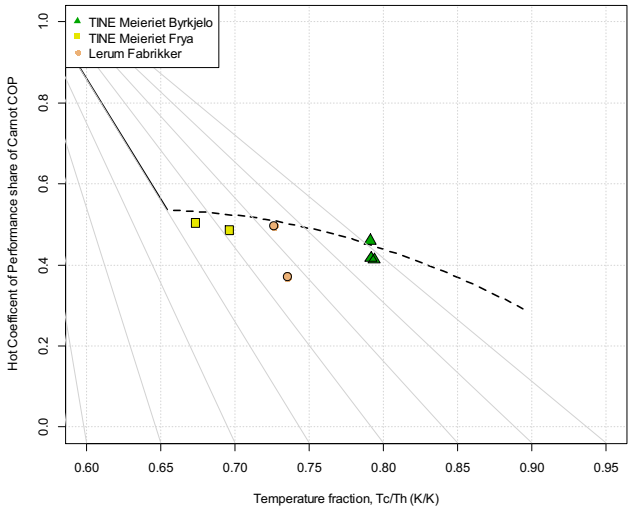

Fig.17. Performance of the SPP-4-106 heat pumps at 3 installations with different operating conditions.

References

1. T. Finkelstein, A.J. Organ, *Air Engines*, ASME Press (2001)
2. Moran and Shapiro, *Fundamentals of Engineering Thermodynamics*, 2nd ed., John Wiley & Sons (1993)
3. Walker et al., *The Stirling Alternative: Power Systems, Refrigerants and Heat Pumps*, CRC Press (1994)
4. B. Hoegel & al., *Theoretical investigation of the performance of an Alpha Stirling engine for low temperature applications*, ISEC 2012 The International Stirling Engine Conference (2012)
5. T.M. Tveit and A. Høeg, *Performance analysis and verification of a novel high temperature difference heat pump*, 11th IEA Heat Pump Conference, Montréal, Canada (2014)
6. D. Gedeon, *SAGE User's Guide, Stirling, Pulse-Tube and Low-T Cooler Model Classes,* Gedeon Associates (2009)
7. Martini, *Stirling Engine Design Manual*, 1983 edition, University Press of the Pacific (2004)

8. A. Høeg, T.M. Tveit and T.A. Asphjell, *Mechanical Design of the 4-500 kWth Stirling Cycle Heat Pump SPP 4-106.* ISEC 2016 Proceedings of the 17th International Stirling Engine Conference, UK. (2016)
9. A. Høeg and T.M. Tveit, *Process design for a 4 x 10.6 litre low-temperature Stirling engine*, ISEC 2018 The International Stirling Engine Conference (2018)